Performance Modelling of the Bioelectrochemical Glycerol Oxidation by a Co-Culture of *Geobacter Sulfurreducens* and *Raoultella Electrica*

Fabian Kubannek[+],[a] Simone Thiel[+],[b] Boyke Bunk,[c] Katharina Huber,[c] Jörg Overmann,[c] Ulrike Krewer,[a] Rebekka Biedendieck,*[b] and Dieter Jahn[b]

An effectively operating microbial electrolysis cell requires an inexpensive electron donor in combination with a defined and stable electron-transferring microbial community. Here, a defined co-culture of *Raoultella electrica* and *Geobacter sulfurreducens* was established to generate current during glycerol oxidation. Maximum current densities of 0.20 mA cm^{-2} and coulombic efficiencies of 21% were achieved. Glycerol metabolization into acetate by *R. electrica* and further acetate utilization by the current-producing *G. sulfurreducens* were detected. Based on these observations, a physico-chemical model was established and used to describe quantitatively the relationships between current density, metabolite concentrations and bacterial growth. The competition for acetate between *G. sulfurreducens* and *R. electrica* was identified as the major limitation of the system. This detailed quantitative understanding of the physiological interactions opens the door for target-oriented genetic engineering of the microbes.

1. Introduction

Microbial fuel cells (MFC) and microbial electrolysis cells (MEC) have emerged as promising and sustainable techniques to produce bioenergy in form of molecular hydrogen or directly as electrical current from low-cost, but often complex undefined substrates such as sewage[1] starch[2] or corn stover biomass.[3] Mostly, microbial communities employed for MFCs or MECs are derived from anaerobic sludge, domestic wastewater or soil samples. The large variability in microbial community composition and the available substrates usually prevents the establishment of stable, reproducible and sustainable biotechnological processes. Alternatively, defined consortia of bacteria with complementary metabolic functions utilizing inexpensive waste products provide a promising alternative. Crude glycerol as the main by-product of the biodiesel industry provides an attractive candidate for a rather defined substrate as it became a cheap feedstock due to the growing global demand for biodiesel.[4] Nevertheless, after the segregation of the fatty acid methyl esters of the biodiesel, the residual crude glycerol is usually contaminated with water, methanol, soap, non-glycerol organic matter and residues of alkaline catalysts[5] resulting in glycerol contents between 23%[6] and 80%.[7] It is obvious that studies with these varying glycerol concentrations are difficult to compare and to reproduce. So far, pure glycerol is mainly used as electron donor in MFC and MEC experiments. However, it has already been demonstrated that crude glycerol can also be used for bioelectrochemical processes.[8] The utilization of glycerol was solely achieved with complex, mostly undefined microbial communities derived from wastewater plants and soil.[9–13] During these processes coulombic efficiencies (CE) between 20% and 50% were achieved.[9,10,14] However, electrochemically active biofilms from wastewater or other undefined sources require enrichment prior use. The electroactive and glycerol consuming microorganisms usually need several weeks to accumulate at the anode or alternatively to produce mediators in the planktonic phase that finally lead to low initial CEs.[9] In order to increase cell concentrations at the anode, biofilms enriched on the electrode surface are usually scraped off and transferred to new MFCs.[15,16] Alternatively, enriched cultures from previous experiments were reused for new experiments.[10] Especially the latter procedure is used to reduce the required time for establishing the bacterial communities. However, the metabolic pathways involved in glycerol-oxidation are difficult to disentangle due to the high diversity of microbial communities. As a result, a targeted optimization of the process is difficult.

Pure bacterial cultures may help to overcome these obstacles. However, the model bacteria for current production

[a] Dr. F. Kubannek,[+] Prof. Dr. U. Krewer
Institute of Energy and Process Systems Engineering
Technische Universität Braunschweig
Franz-Liszt-Straße 35, 38106 Braunschweig, Germany
[b] S. Thiel,[+] Dr. R. Biedendieck, Prof. Dr. D. Jahn
Institute of Microbiology
Braunschweig Integrated Centre of Systems Biology (BRICS)
Technische Universität Braunschweig
Rebenring 56, 38106 Braunschweig, Germany
E-mail: r.biedendieck@tu-braunschweig.de
[c] Dr. B. Bunk, Dr. K. Huber, Prof. Dr. J. Overmann
Leibniz Institute DSMZ-German Collection of Microorganisms and Cell Cultures GmbH
Inhoffenstraße 7B, 38124 Braunschweig, Germany
[+] These authors contributed equally to this work.

Supporting information for this article is available on the WWW under https://doi.org/10.1002/celc.202000027

localized at the anode, *Geobacter sulfurreducens* and *Shewanella oneidensis*, are not capable of metabolizing glycerol naturally[17,18] but when genetically modified.[19] Alternatively, other (genetically engineered) bacterial strains such as *Pseudomonas aeruginosa* ATCC 27853,[20] *Escherichia coli* ATCC 27325[21] and DH5αZ1[22] *Klebsiella pneumonia* L17[23] or *Bacillus subtilis* BBK006[24] were used in MFCs to convert glycerol as electron donor to pyocyanin or electricity. Furthermore, a few studies investigated the potential of defined co-cultures in MFCs or MECs for the glycerol-derived production of 1,3-propanediol as a building block for industrial polymer production, often with the simultaneous production of ethanol,[25] or hydrogen,[26] or electrical current.[24,27,28] So far, most approaches struggled with lower CEs compared to those of the bioelectrochemical glycerol-oxidation by biofilms enriched from undefined microbial communities. In order to optimize the efficiency of defined co-cultures in MFCs and MECs, a better understanding of the underlying electron transfer mechanisms and the identification of possible process limiting parameters are therefore needed. *G. sulfurreducens* is a suitable partner for establishing defined co-cultures, because its electron donor spectrum is well known.[17,29] Furthermore, its current production from acetate is higher than the bioelectrochemical performance of enrichment cultures.[30] However, due to its inability to use glycerol as electron donor, additional partner organisms converting glycerol to acetate are required. *Raoultella electrica* was identified as a promising candidate for the glycerol conversion. *R. electrica* DSM 102253^T was originally isolated from a glucose-fed anodic biofilm.[31] Recently, its genome was elucidated and revealed genes potentially involved in glycerol oxidation and acetate formation.[31] Consequently, in the present work, the two Gram-negative bacteria *G. sulfurreducens* DSM 12127^T and *R. electrica* DSM 102253^T were investigated in a bioelectrochemical reactor using pure glycerol as electron donor. Metabolic interactions during the co-cultivation of both bacteria were characterized. Based on the observed results, a mathematical simulation model was established to gain quantitative insights into the biochemical processes in the reactor. Rate constants of the biofilm and planktonic cell growth were determined and kinetic expressions for substrate consumption and metabolite production were formulated. Further, the simulation model was used to identify limitations of the co-cultivation regarding current production. Finally, the development of strategies to increase the current density and the CE by targeted metabolic engineering or process adjustments such as changing the composition of the initial inoculum are outlined.

2. Results and Discussion

2.1. *R. Electrica* Utilizes Glycerol as Electron Donor in Bioelectrochemical Processes

In order to identify bacteria capable of glycerol utilization in bioelectrochemical processes, enrichment experiments were conducted in an MEC using a defined medium with pure glycerol as electron donor and wastewater as inoculum. V3 amplicon sequencing of the resulting bacterial community revealed an enrichment of *Raoultella* species up to 1.4% and 6.8% in primary, secondary and tertiary biofilms and in the planktonic bacterial fraction, respectively (Figure S1). In the next step, the type strain *R. electrica* DSM 102253^T was successfully tested for glycerol utilization with the production of acetate and formate (Figure S2). Consequently, *R. electrica* DSM 102253^T was chosen for co-culture experiments with *G. sulfurreducens* DSM 12127^T to allow for the glycerol-dependent current production.

2.2. Co-cultures of *R. Electrica* and *G. Sulfurreducens* Oxidize Glycerol with the Formation of Current at the Anode of an MEC

To investigate the current production from glycerol, biological triplicates in MECs with a three-electrode setup were inoculated with pure cultures of *R. electrica* and *G. sulfurreducens*. The co-cultures of *R. electrica* and *G. sulfurreducens* successfully produced current by bioelectrochemical glycerol oxidation (Figure 1). In control experiments, none of the individual bacteria was able to produce significant amounts of current when tested alone in this set-up (Figure S3). Additionally, co-cultures of *R. electrica* and *G. sulfurreducens* were cultivated in control experiments without an applied potential under anoxic conditions. Since under these so-called open circuit conditions no electron acceptor in form of a charged electrode was available for *G. sulfurreducens*, only planktonic growth of *R. electrica* was assumed. As explained in detail below, resulting composition of metabolites of the co-cultures under open and closed-circuit conditions (Figure 2) allowed the identification of the metabolic pathways connected to current production by the co-culture of *R. electrica* and *G. sulfurreducens*.

Maximum current densities of 0.19 mA cm^{-2} (replicate 1), 0.22 mA cm^{-2} (replicate 2) and 0.20 mA cm^{-2} (replicate 3) were achieved, respectively (Figure 1b). All curves representing the current densities showed varying slopes during the cultivation time with plateaus between 25 and 50 h and 75 and 100 h. This diauxic behavior might be the result of shifts between utilized carbon sources by *R. electrica* which might cause transient limitations of the availability of acetate for *G. sulfurreducens*. The current densities dropped sharply within 5 to 12 hours after their maximum peaks indicating that all electron donors were consumed.

In previous experiments, the co-culture of *S. oneidensis* MR-1 and *K. pneumoniae* J2B on 100 mM glycerol reached a maximum voltage of approx. 22.6 mV and a maximum current density of 12.3 mA m^2, corresponding to 1.23 μA cm^{-2} in an MFC.[27] This maximum current density was significantly lower than the maximum current density achieved by our co-culture. Finally, a maximum current of 1.34 mA, that corresponded to a current density of 0.11 mA cm^{-2}, was generated by a co-culture with *G. sulfurreducens* DSM 12127^T and *Clostridium cellobioparum* ATCC 15832^T in an MEC. This co-culture was supplied with approx. 150 mM glycerol at an anode potential of 0.24 V vs. Ag/AgCl, which is comparable to our anode potential at 0.2 V vs.

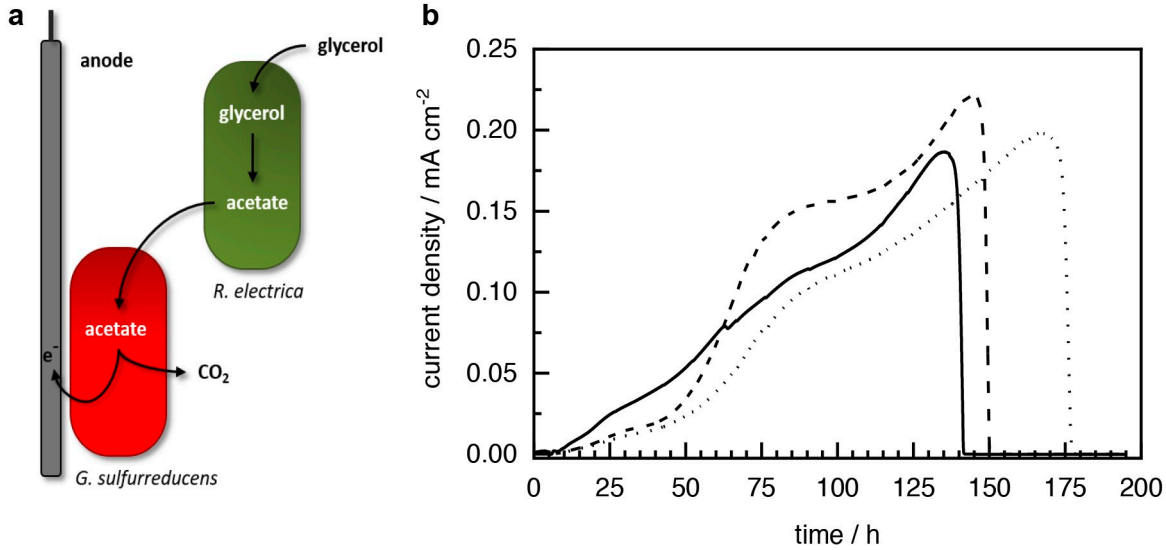

Figure 1. Current production by the co-cultures of *R. electrica* and *G. sulfurreducens*. Shown are a simplified scheme of the metabolic processes underlying the current production from glycerol by the co-culture (a) and the current production from 20 mM glycerol (b). The current densities over time resulting from three independent co-cultivations are depicted. The solid line represents replicate 1, the dashed line replicate 2, the dotted line replicate 3. The anode potential was 0.2 V vs. Ag/AgCl.

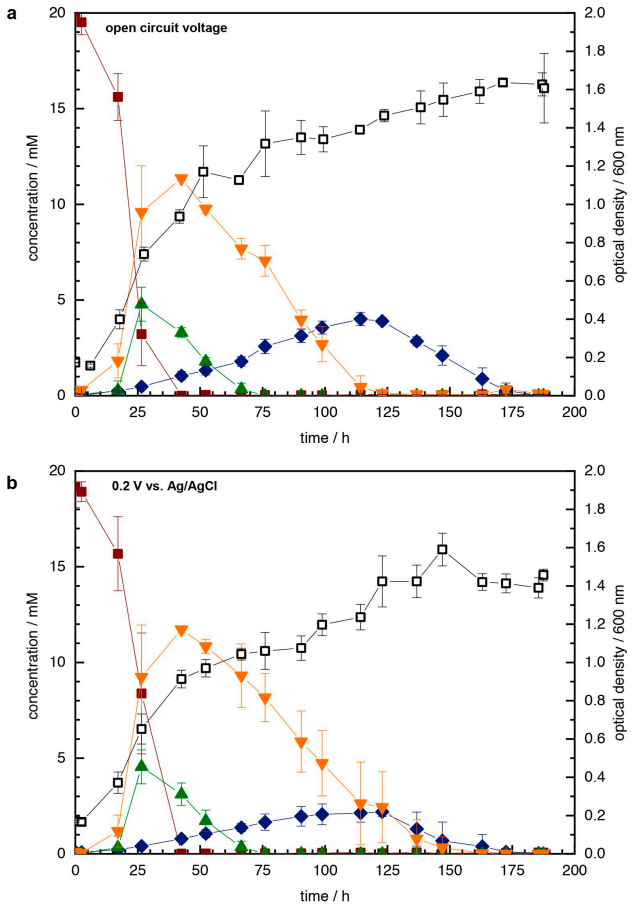

Figure 2. Composition of metabolites of co-cultures of *R. electrica* and *G. sulfurreducens* grown in open circuit (a) and closed circuit (b) setups. Shown are the optical densities determined at 600 nm (□) of planktonic cells and the extracellular measured concentrations of glycerol (■), acetate (♦), formate (▲) and ethanol (▼). Mean values and standard deviations of the replicates shown in Figure 1 are displayed.

Ag/AgCl.[25] Overall, the setup used in this investigation resulted in the highest maximum current densities using the lowest concentration of glycerol.

Next, CEs of 17.9% (replicate 1), 20.6% (replicate 2) and 21.0% (replicate 3) were determined. These values are in the same range as the CE of 23.08% determined for a glycerol-fed pure culture of *Bacillus subtilis* BBK006[24] or the CEs of 14–27% for undefined mixed cultures.[10,32] However, some undefined mixed cultures achieved even higher CEs of up to 35%.[9,33,34] Electron losses were described before to be the result of the production of metabolites that do not contribute to current production.[35] Thus, most of the electrons were probably used for biomass production by *R. electrica* and the production of ethanol. Later maintenance might also contribute to electron consumption (Figure S10). Assuming that *R. electrica* converted formate to CO_2 and H_2, electrons were transferred to H_2 and contributed to lowering the CE. Finally, the charge balance was considering an assumed average biomass constitution to calculate the charge used for biomass production, and the degree of reduction of the biomass might be different from what we assumed.

2.3. Metabolic Principles Underlying Glycerol-Driven Current Production by the Co-Culture of *R. Electrica* and *G. Sulfurreducens*

To investigate the metabolic interaction between *R. electrica* and *G. sulfurreducens* regarding cell growth and substrate conversion, samples were taken at different time points. The optical density at 600 nm (OD_{600}) of the planktonic phase and the concentrations of glycerol and resulting organic acids were measured (Figure 2). Additionally, we calculated carbon and electron balances for two different time points during the

cultivations (after 26.5 hours when glycerol was still present and at 114.25 hours at the highest concentration of acetate). Glycerol was completely depleted after 42 hours by *R. electrica* in all co-cultures both with and without potential (Figure 2). Simultaneously, the OD_{600} of planktonic cells increased rapidly up to 0.91 ± 0.046 (0.2 V vs. Ag/AgCl, closed circuit conditions) and 0.94 ± 0.035 (open circuit conditions).

In order to understand the metabolic processes performed by *R. electrica* during glycerol utilization, metabolic profiles were recorded under open circuit conditions, when *G. sulfurreducens* did not consume compounds formed by *R. electrica*. Under open circuit conditions, the co-cultures of *R. electrica* and *G. sulfurreducens* showed a composition of metabolites of a typical mixed acid fermentation, producing the three main metabolites ethanol, formate and acetate (Figure 2a). Neither lactate nor succinate were detected. Since *R. electrica* is missing the *dhaB* gene in its genome it should not be capable of producing 1,3-propandiol.[31] Once the provided primary carbon source glycerol was depleted, formate and ethanol were re-imported and utilized. Correspondingly, their concentrations decreased. A maximum formate concentration of 4.78 ± 0.89 mM was detected after 26 hours before it was completely converted by *R. electrica* to CO_2 and H_2. The acetate concentration still increased after the depletion of glycerol and the OD_{600} increased steadily up to 1.39 ± 0.02 after 114 hours. Since *G. sulfurreducens* is not able to use ethanol as an electron donor it cannot be responsible for the decreasing ethanol concentration.[36,37] Hence, it can be assumed that *R. electrica* oxidized all of the previously produced ethanol (11.36 ± 0.11 mM) to acetate in order to gain energy. When all ethanol was consumed after 123 hours, the acetate concentration decreased, indicating that *R. electrica* now also re-imported and metabolized the previously formed acetate. The latter was consumed completely after 171 hours resulting in a final OD_{600} of 1.64 ± 0.02. After the consumption of acetate, all carbon sources were depleted resulting in a constant OD_{600} until the end of the experiment.

Under closed circuit conditions, the time-resolved variations in the concentrations of all metabolites apart from acetate were found to be very similar compared to open circuit conditions (Figure 2b). However, Speers *et al.* (2012) showed that *G. sulfurreducens* is capable of using formate as an electron donor for current production, additionally stimulated by the presence of acetate.[29] Hence, a small amount of the detected formate (4.55 ± 0.88 mM) might also be consumed by the electroactive *G. sulfurreducens* biofilm, in addition to the conversion of formate to CO_2 and H_2 by *R. electrica*. However, the differences between the formate concentrations in the presence and absence of electrical potential were insignificantly small, indicating that *G. sulfurreducens* mainly used acetate as electron donor for current generation. The determined ethanol concentrations were very similar to those of the co-cultures under open circuit conditions with a maximum concentration of 11.72 ± 0.19 mM after 42 hours. Most likely, this was again converted to acetate by *R. electrica* resulting in a high acetate availability for the now metabolically active and current-producing *G. sulfurreducens* biofilm.

Due to the acetate consumption by both species, its concentration was lower under closed circuit than under open circuit conditions. However, an acetate accumulation of up to 2.19 ± 0.24 mM was detected after 123 hours, possibly caused by a limited metabolic exchange capacity of the *G. sulfurreducens* biofilm at the anode surface.[25] Besides, the pH value effects the bioelectrochemical performance and growth of *G. sulfurreducens*.[38] It was shown that pH changes from 6.5 to 7 led to an increase of the current density of undefined mixed bioelectrochemical biofilms of 20%.[39] The initial pH in the medium of our co-culture was 6.96 and dropped to 6.26 after 26.5 hours (Figure S6). However, it increased quickly again and a pH value of 6.57 after 42 hours was measured. During the accumulation of acetate from 50 to 123 hours the pH fluctuated between approx. 6.6 and 6.7. Therefore, the performance of the electrochemical biofilm was probably not optimal compared to the initial cultivation conditions and could be also responsible for the accumulation of acetate. After 150 hours all of the ethanol was depleted, followed by a decline in acetate concentration. After the residual acetate was depleted, the current density dropped sharply. A slow decline of the OD_{600} values started (Figure 2b). The determined dry biomass of the biofilm at the end of the cultivation was 10.57 mg (replicate 1), 6.00 mg (replicate 2) and 10.57 mg (replicate 3), respectively. Ten mg of biomass with an approximate biofilm density ρ_{BF} of 40–200 mg cm^{-3}[40] should result in a biofilm thickness of 10-50 μm in our experiments. This is comparable to acetate-fed *G. sulfurreducens* biofilms of 66 and 49 μm thickness which have been detected on graphite electrodes after the first and second batch cycle.[41] Unexpectedly, the current profiles of the three replicates did not show any significant differences.

The experimental carbon and electron balances (Figure S4 and Figure S5) illustrated that electron and carbon losses increased during the time of cultivation. One possible reason for that could be a change in the biofilm mass, which was not measured at these time points. Additionally, volatile compounds were not considered for these calculations. However, a simulation model could be used to quantify a part of the missing carbon and electrons. All experimental results indicated that the co-culture of *R. electrica* and *G. sulfurreducens* transferred electrons rather via metabolites (i.e. acetate) than via a direct interspecies electron transfer. As the glycerol consumption remained almost identical between open and closed circuit conditions and the OD_{600} of the planktonic phase was even higher at open circuit conditions, the interaction between *R. electrica* and *G. sulfurreducens* was probably not mutualistic. Most importantly, current production from glycerol oxidation was only enabled by the co-culture and not by pure single cultures, indicating cooperativity of both bacteria.

2.4. Genome-Deduced Metabolic Pathways for the Glycerol-Based Current Production by the Co-Culture of *R. Electrica* and *G. Sulfurreducens*

The obtained experimental data outlined above were combined with genomic data from *R. electrica*[31] and from

G. sulfurreducens.[29,42,43] Possible metabolic pathways from glycerol oxidation to current production by the co-culture of *R. electrica* – *G. sulfurreducens* were deduced and are illustrated in Figure 3.

After glycerol uptake and phosphorylation, conversion to pyruvate by *R. electrica* employing glycolysis enzymes is most likely. Next, the pyruvate formate lyase (PFL), which is only active under anaerobic conditions, can catalyze the reaction of pyruvate to acetyl-CoA and formate. Correspondingly, accumulation of formate was detected in the medium early in the cultivation (Figure 2) before it was again depleted either by converting it into CO_2 and H_2 using the formate hydrogen lyase complex (FHL) or through the uptake by *G. sulfurreducens* cells. Murarka *et al.* (2008) demonstrated that ethanol is essential during glycerol fermentation by different *E. coli* strains, as one mol of ATP is generated from the conversion of one mol glycerol to ethanol in a redox-balanced process.[45] The high concentrations of ethanol detected in our co-cultures are consistent with these observations. Furthermore, the ethanol-generating pathway was utilized in the reverse direction to produce acetate once glycerol was depleted. Acetate conversion in turn leads to the generation of one ATP. During acetate production from ethanol, acetyl-CoA gets converted to acetyl-phosphate by the phosphate acetyltransferase (PTA) and subsequently into acetate by the acetate kinase (AK) with the formation of one ATP. Finally, acetate was secreted into the medium. Once all ethanol was consumed, acetate from the medium was re-imported and re-used by the acetyl-CoA synthetase (ACS) with the consumption of one ATP.

However, most of the acetate was imported and utilized by *G. sulfurreducens*. The pathways of *G. sulfurreducens* displayed in Figure 3 were based on the *in silico* predictions of the central metabolism by Meng *et al.* (2013) and genomic data.[29,42,43] After the uptake of acetate and its conversion into acetyl-CoA, which enters the incomplete TCA cycle, eight electrons per acetate molecule must be released and transferred to the anode by direct extracellular electron transfer mechanisms. Speers *et al.* (2012) found that *G. sulfurreducens* is capable of using formate as electron donor for current production. The corresponding reaction is catalyzed by the formate dehydrogenase (FDH) with the release of two electrons per molecule of formate.[29] However, in the presence of acetate, as in our co-cultures, formate can also be used for the production of cell biomass. In particular, pyruvate formate lyase (PFL) can convert the available formate to pyruvate, which can then be used as a building block in certain anabolic processes in *G. sulfurreducens*.[29] In our experimental data, there was no significant difference in the formate concentrations between open and closed circuit conditions. Consequently, the main current production by the co-culture of *R. electrica* and *G. sulfurreducens* was due to acetate oxidation.

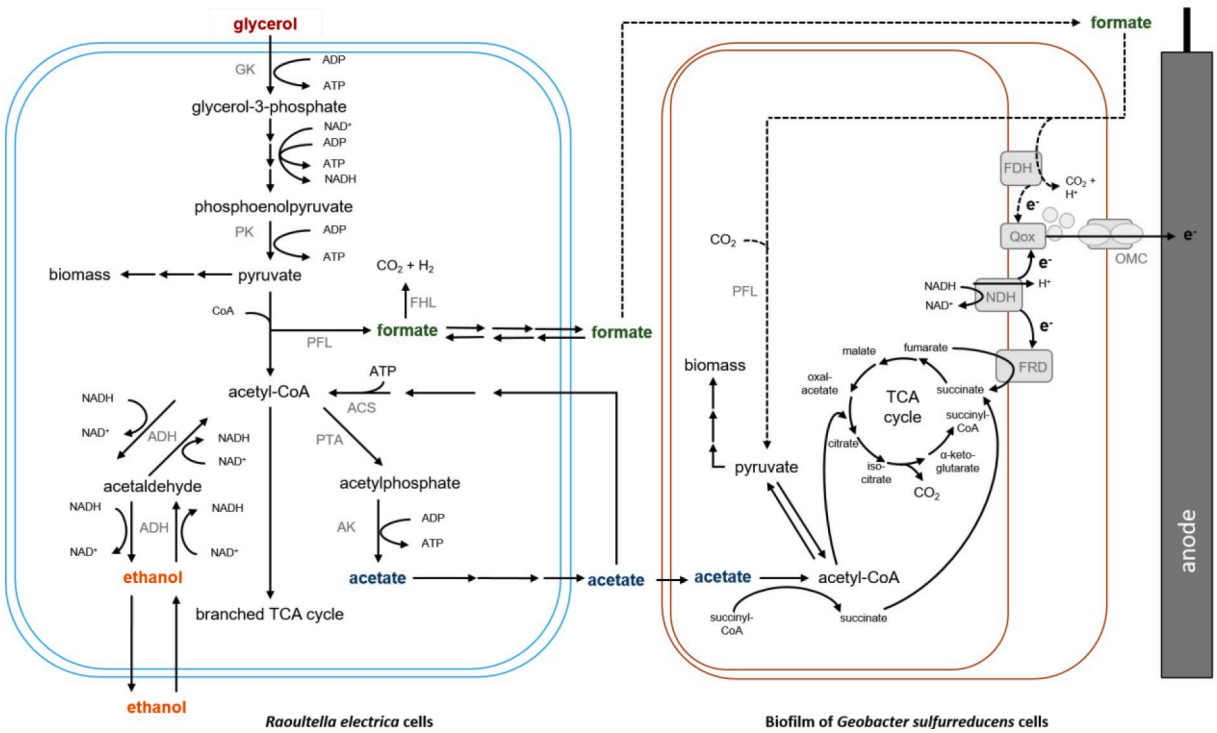

Figure 3. Scheme of the metabolic pathways from glycerol-oxidation to current production by the co-culture of *R. electrica* – *G. sulfurreducens*. Genomic data from Thiel *et al.* (2019),[31] Methé *et al.* (2003),[43] Speers *et al.* (2012)[29] and Meng *et al.* (2013)[42] were combined for the deduction of shown pathways. ACS: acetyl-CoA synthetase, ADH: alcohol dehydrogenase, AK: acetate kinase, FDH: formate dehydrogenase, FHL: formate hydrogen-lyase, FRD: fumarate reductase; GK: glycerol kinase, NDH: NADH dehydrogenase; OMC: outer membrane cytochromes; PFL: pyruvate formate lyase, PK: pyruvate kinase, PTA: phosphate acetyltransferase; Qox: one of two putative quinol oxidases.[44]

2.5. Modelling

In order to obtain a quantitative understanding of the experimental data with a carbon mass balance for the entire reactor process, a physico-chemical simulation model was constructed. This model aims at describing the major conversion steps that dominate the current production of our co-cultures to identify the rate limiting steps. Consequently, the conversion reactions of the main metabolites glycerol, ethanol, formate, and acetate were included. Compounds that were only found in minor amounts during the experiments or were obviously not involved in current production were not considered.

Due to the rapid stirring in the reactor, a homogenous liquid phase was assumed. The uptake and secretion of metabolites by the bacteria are usually fast and not rate limiting. Consequently, any conversion directly affects the metabolite concentrations of the reactants. The following balance equations describe the production and consumption rates of dissolved compounds:

$$\frac{dc_{gly}}{dt}V = -r_{gly,et} - r_{gly,ac} \quad (1)$$

$$\frac{dc_{et}}{dt}V = (1 - f_{0,gly})r_{gly,et} - r_{et,ac} \quad (2)$$

$$\frac{dc_{fo}}{dt}V = (1 - f_{0,gly})(r_{gly,ac}+r_{gly,et}) - r_{fo,en} - r_{fo,bf} \quad (3)$$

$$\frac{dc_{ac}}{dt}V = \left(1 - f_{0,gly}\right)\, r_{gly,ac} + \left(1 - f_{0,et}\right)r_{et,ac} - r_{ac,en} - r_{ac,bf} \quad (4)$$

with $r_{i,j}$ denoting the conversion rate from species i to j and the indices gly = glycerol, et = ethanol and ac = acetate. $r_{ac,en}$ is the rate of endogenous acetate consumption, $r_{ac,bf}$ is the rate of bioelectrochemical acetate oxidation by the biofilm, V is the reactor volume, $f_{0,gly}$ and $f_{0,et}$ are the shares of carbon utilized for biomass growth in the liquid phase on glycerol or ethanol, respectively. It is assumed that this share is constant independent of the product. Equation (1) is the glycerol mass balance. Glycerol is not produced in the reactor but converted to ethanol or acetate in the liquid phase. In both cases also one molecule of formate is produced per molecule of acetate or ethanol. Equation (2) is the ethanol mass balance. Due to the formation of biomass, less than one molecule of ethanol is produced per molecule of glycerol consumed. Equation (3) is the formate mass balance. One molecule of formate is produced along with every molecule of ethanol or acetate in the liquid phase. Formate is consumed by the biofilm or by the bacteria in the liquid phase. Equation (4) is the acetate mass balance. Acetate is produced in the liquid phase from glycerol or ethanol. In both cases part of the carbon is used for the formation of biomass so that less than one molecule of acetate is produced per molecule of glycerol or ethanol that is consumed. Acetate consumption takes place in the liquid phase and in the biofilm.

As described above, G. *sulfurreducens* grew only on the electrode with the anode as the sole electron acceptor. No planktonic growth was observed. Consequently, G. *sulfurreducens* oxidized acetate or formate solely electrochemically, while all other conversions were performed in the liquid phase by *R. electrica*. The growth of the biofilm biomass X_{bf} (solely *G. sulfurreducens)* and the planktonic biomass X_{lq} (solely *R. electrica)* are described by the following balance equations [Equations (5) and (6)]:

$$\frac{dX_{bf}}{dt} = M_{bf}f_{0,bf}(2r_{ac,bf} + r_{fo,bf}) \quad (5)$$

$$\frac{dX_{lq}}{dt} = M_{lq}(3f_{0,gly}r_{gly,et}+3f_{0,gly}r_{gly,ac}+2f_{0,et}r_{et,ac} + 2f_{0,ac}r_{ac,en}) \quad (6)$$

Here $f_{0,bf}$ is the share of carbon utilized for biofilm growth and $f_{0,i}$ is the share of carbon utilized for growth of the planktonic biomass utilizing substrate *i*. Molar masses for the biomass of the biofilm (M_{bf}) and in the liquid phase (M_{lq}) were normalized by the number of carbon atoms, assumed to be equal and set to 24.6 g mol^{-1}.[46] As described above, *G. sulfurreducens* produced biomass from both formate and acetate while *R. electrica* produced biomass from glycerol, ethanol and acetate. The formate consumed in the planktonic phase was entirely converted into CO_2.

The value of $f_{0,bf}$ is not a constant. It depends on the biofilm biomass [Equation (7)]:

$$f_{0,bf} = f_{0,bf,0}\frac{X_{bf,0}}{X_{bf}} \quad (7)$$

This relation allows to describe a non-exponential but linear growth of the biofilm. Linear growth was chosen not based on physical considerations but because the development of the measured current density is linear rather than exponential. Growth for *G. sulfurreducens* that proceeded linearly after an initial phase was observed before,[47,48] however, without any explanation.

The rates of acetate and formate consumption by the biofilm $r_{ac,bf}$ and $r_{fo,bf}$ are modelled via the Nernst-Monod equation [Equations (8) and (9)]:[40]

$$r_{ac,bf} = q_{max,bf,ac}X_{bf}\frac{c_{ac}}{c_{ac} + K_{S,ac,bf}} \frac{1}{1 + \exp(-FR^{-1}\, T^{-1}(E - E_{KA}))}k^{lag,bf} \quad (8)$$

$$r_{fo,bf} = q_{max,bf,fo}X_{bf}\frac{c_{fo}}{c_{fo} + K_{S,fo,bf}} \frac{1}{1 + \exp(-FR^{-1}\, T^{-1}(E - E_{KA}))}k^{lag,bf} \quad (9)$$

where $q_{max,bf,ac}$ and $q_{max,bf,fo}$ are the specific maximum substrate conversion rates of acetate and formate by the biofilm, $K_{S,ac,bf}$ and $K_{S,fo,bf}$ are the respective half-saturation rate constants, F is the Faraday constant and T the temperature. The half-saturation

potential E_{KA} is set to -0.35 V[40] so that the difference between the electrode potential E and E_{KA} is large enough to avoid a limitation of the bacterial activity. The lag phase factor $k^{lag,bf}$, which was not present in the original form of the equation, was introduced to describe the lag phase resulting from the adaptation process to the new medium and the initial attachment to the electrode by *G. sulfurreducens*. It was not resolved in detail and is defined as [Equation (10)]:

$$k^{lag,bf} = \frac{t}{t + k^{lag,bf,0}} \tag{10}$$

where t is the time and $k^{lag,bf,0}$ is a constant describing the length of the lag phase. This approach is simple compared to models found in the literature which focus on a detailed description of the lag phase.[49] Yet it allows to model a smooth transition between lag phase and exponential growth phase with introduction of only one additional model parameter.

The current density i is calculated by Equation (11):

$$i = \left(1 - f_{0,bf}\right)\left(8r_{ac,bf} + 2r_{fo,bf}\right) FA^{-1} \tag{11}$$

where A denotes the electrode area, and the factors 8 and 2 are the numbers of electrons released per molecule of oxidized of acetate and formate according to the net reaction equations [Equations (12) and (13)]:

$$CH_3COO^- + 2H_2O \rightarrow 8e^- + 7H^+ + 2CO_2 \tag{12}$$

$$HCOO^- \rightarrow 2e^- + H^+ + CO_2 \tag{13}$$

The conversion rates in the planktonic phase are described by Monod kinetics. The rate of conversion from metabolite i to j is $r_{i,j}$, which is calculated from the following [Equation (14)]:

$$r_{i,j} = q_{max,i,j} X_{lq} \frac{c_i}{c_i + K_{S,i,j}} k^{lag,lq} \tag{14}$$

As for the biofilm, a lag phase factor for the planktonic phase $k^{lag,lq}$ was added to describe the initial lag phase during which the bacteria adjust to the new medium [Equation (15)]:

$$k^{lag,lq} = \frac{t}{t + k^{lag,lq,0}} \tag{15}$$

$k^{lag,lq,0}$ is a constant describing the length of the lag phase. The values for the fixed model parameters, which are based on experimental data or were drawn from the literature, are shown in Table 1. Initial values for the concentrations $c_{0,i}$ are set to the measured concentration of the first sample that was taken directly after inoculation of the reactor. The initial amount of the planktonic *R. electrica* biomass $X_{0,lq}$ was calculated from the OD_{600} of the *R. electrica* inoculum using an experimental correlation of OD and CDW. The initial amount of the *G. sulfurreducens* biomass in the biofilm was zero at the beginning of the experiment. However, in the model a finite amount of initial biofilm biomass $X_{0,bf}$ is considered to avoid the need of describing the stochastic initial attachment process of *G. sulfurreducens* cells on the graphite surface.

Table 1. Fixed model parameters and initial values.

Parameter	Value	Notes
A [m^2]	5×10^{-3}	From experimental data
E_{KA} [V]	−0.35	Ref. [40]
F [$C\,mol^{-1}$]	96485	–
R [$J\,mol^{-1}\,K^{-1}$]	8.3144	–
T [K]	308.18	From experimental data
V [L]	0.5	From experimental data
M_{lq} [$kg\,mol^{-1}$]	0.0246	[46]
M_{bf} [$kg\,mol^{-1}$]	0.0246	[46]
$c_{0,gly}$ [$mol\,m^{-3}$]	20	From experimental data
$c_{0,et}$ [$mol\,m^{-3}$]	0	From experimental data
$c_{0,ac}$ [$mol\,m^{-3}$]	0.1	From experimental data
$c_{0,fo}$ [$mol\,m^{-3}$]	0	From experimental data
$X_{0,bf}$ [kg]	Identified from experimental data (Table 2)	
$X_{0,lq}$ [kg]		From experimental data

The model equations were implemented in the software MATLAB. A parameter identification procedure was carried out similarly to Kubannek and Krewer (2019)[50] to minimize the deviation between the model output and the third triplicate. Details are explained in the Supporting Information.

2.6. Reaction Rates and Limitations

The simulated and experimental values for current densities, metabolite concentrations and biomasses are depicted in Figure 4. They show a good agreement between experimental and simulated data.

The model accurately describes the fast decrease of the glycerol concentration, the subsequent production of ethanol and formate, the gradual consumption of ethanol and the linear increase in current density. This observation indicates that the model equations are suitable to describe the main processes in the bioelectrochemical reactor. A deviation between experimental and simulated data can be observed regarding the biomass growth in the planktonic phase, which was overestimated in the beginning of the simulation and then dropped to almost zero after 50 hours. In this respect, the model failed to reproduce the experimental data since under open circuit conditions growth from acetate consumption was observed. One reason might be the fact that an acetate accumulation inside the bacterial cells was not considered. In addition, the OD-CDW correlation might differ between the cells in exponential and stationary phase of growth. However, the measured biomass of the biofilm correlated quite well with the simulation result.

Figure 5a shows the conversion rates over time. The glycerol conversion rate to ethanol increased rapidly, reached a maximum at approximately 40 hours and dropped to zero once all glycerol was consumed. The conversion rate of ethanol to acetate increased rapidly in the initial phase with an increasing ethanol concentration followed by a slow rise until all ethanol was consumed after 162 hours. Bioelectrochemical acetate oxidation in the biofilm increased linearly with the biofilm

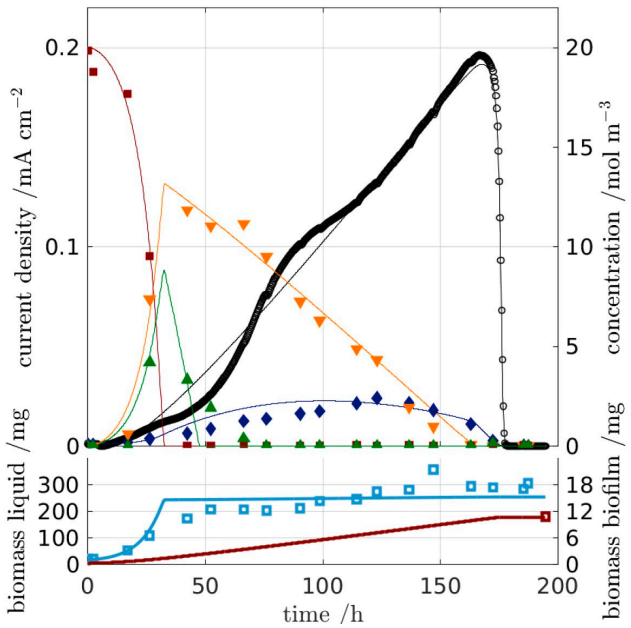

Figure 4. Comparison of experimental (lines) and simulated (symbols) values of current densities, metabolite concentrations and biomasses for the third replicate. Shown are the current densities (○), the liquid phase biomass obtained from the optical densities of planktonic cells determined at 600 nm (□), the biofilm biomass determined at the end of the experiment (□), and the measured concentrations of glycerol (■), acetate (♦), formate (▲) and ethanol (▼).

biomass until all acetate was consumed after 180 hours. The competing endogenous acetate consumption in the liquid phase first increased rapidly with increasing acetate concentration, reached a maximum at 100 hours and then decreased with the falling acetate concentration. The rates of endogenous and bioelectrochemical acetate consumption were in the same order of magnitude. Between approximately 50 and 150 hours the difference between the acetate production rate from ethanol and the sum of the two consumption rates were low, leading only to moderate changes in the acetate concentration despite the large consumption rates. The conversion rates from glycerol to acetate in the planktonic phase and from formate to CO_2 in the biofilm were always zero.

Figure 5b shows the total carbon mass balance for the bioelectrochemical reactor presenting the amount of carbon atoms in form of metabolites, biomass or CO_2 at any time point during the cultivation. The amount of carbon in the metabolites was calculated by multiplying their concentrations with the number of carbon atoms per molecule and the reactor volume. The carbon in the planktonic and biofilm biomass was calculated by dividing the biomass by the molecular weight normalized by the carbon atom. CO_2 formation resulted from the electrochemical oxidation of acetate and endogenous consumption of acetate or formate. Initially, almost all carbon was present in the form of glycerol, which was then converted to ethanol, formate and planktonic biomass (approx. after 42 hours). In the end most of the carbon was present in form of biomass and CO_2 (>150 hours). The amount of carbon in the biofilm was very low at all times (<2 mmol). The reaction rates and the carbon mass balance provided the basis for the identification of strategies to improve the CE.

The identified model parameters are summarized in Table 2. The rates for the direct conversion of glycerol to acetate $q_{max,gly,ac}$ and for the bioelectrochemical oxidation of formate $q_{max,bf,fo}$ were both predicted to be zero. Thus, even though these two pathways were possible according to genome data,

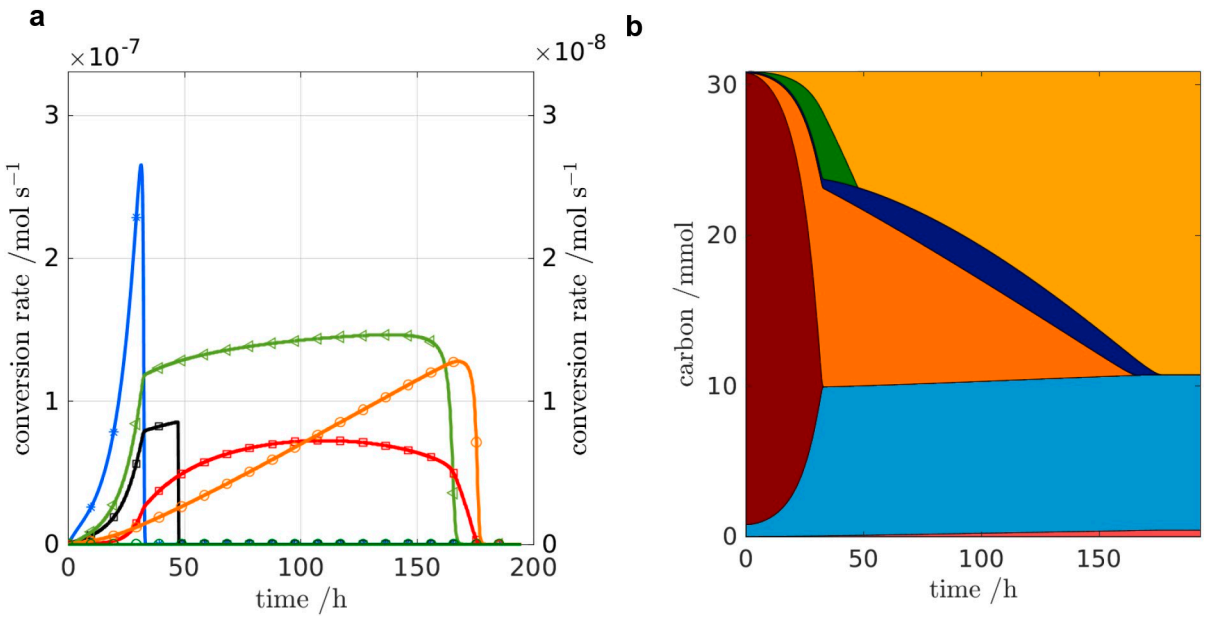

Figure 5. a) Simulated reaction rates of metabolite production and consumption. Legend entries correspond to the reaction rates used in equations 1–4. Left y-axis: glycerol-to-ethanol (■) and endogenous formate consumption (□). Right y-axis: ethanol-to-acetate (◁), endogenous acetate consumption (□), acetate-to-CO_2 (○), formate-to-CO_2 (○). b) Simulated carbon mass balance. Biofilm biomass (light red), biomass in liquid phase (light blue), glycerol (dark red), ethanol (orange), acetate (dark blue), formate (green), CO_2 (yellow).

Table 2. Model parameters of the mathematical model for the bioelectrochemical oxidation of glycerol. Parameter values were identified from experimental data by maximizing the log-Likelihood function.

Parameter	Value	Note
$q_{max,gly,ac}$ [mol s^{-1} kg^{-1}]	0	
$q_{max,gly,et}$ [mol s^{-1} kg^{-1}]	1.80×10^{-3}	
$q_{max,et,ac}$ [mol s^{-1} kg^{-1}]	6.38×10^{-5}	
$q_{max,ac,en}$ [mol s^{-1} kg^{-1}]	6.00×10^{-5}	
$q_{max,fo,en}$ [mol s^{-1} kg^{-1}]	4.25×10^{-4}	
$q_{max,bf,ac}$ [mol s^{-1} kg^{-1}]	1.39×10^{-3}	Literature: 1.53×10^{-3}[40]
$q_{max,bf,fo}$ [mol s^{-1} kg^{-1}]	0	
$K_{S,gly,ac}$ [mol m^{-3}]	–	Not identifiable ($q_{max,gly,ac}=0$)
$K_{S,gly,et}$ [mol m^{-3}]	0.28	Not identifiable from the data
$K_{S,et,ac}$ [mol m^{-3}]	0.06	
$K_{S,ac,en}$ [mol m^{-3}]	2.00	= upper boundary
$K_{S,fo,en}$ [mol m^{-3}]	2.00×10^{-5}	Not identifiable from the data
$K_{S,bf,ac}$ [mol m^{-3}]	0.04	Literature: 0.03[40]
$K_{S,bf,fo}$ [mol m^{-3}]	–	Not identifiable ($q_{max,bf,fo}=0$)
$f_{0,gly}$/–	0.30	
$f_{0,et}$/–	0	
$f_{0,ac}$/–	0.07	
$f_{0,bf,0}$/–	0.95	= upper boundary
$k^{lag,bf,0}$ [s]	3.6×10^{4}	= upper boundary
$k^{lag,lq,0}$ [s]	3.6×10^{4}	= upper boundary
$X_{0,bf}$ [kg]	3.17×10^{-7}	

their contribution to the overall process was negligible. The maximum substrate consumption $q_{max,bf,ac}$ and half-saturation rates $K_{S,bf,ac}$ for *G. sulfurreducens* agreed well with values found in the literature.[40] That implies that the bioelectrochemical biofilm of our co-culture reacted like a pure *G. sulfurreducens* biofilm. The half-saturation rate constant $K_{S,gly,et}$ could not be identified from the data because the objective function is not sensitive to this parameter. The rate constant for endogenous acetate consumption $q_{max,ac,en}$ reached the lower boundary and the half-saturation rate constant for this conversion step $K_{S,ac,en}$ reached the upper boundary of the allowed parameter interval. The limits of the interval were chosen based on the concentration transients under open circuit conditions, which showed that the endogenous acetate consumption rate could not be very low. This finding indicates that the endogenous acetate consumption rate under open circuit conditions might be higher than under closed circuit conditions. The reason could be an adaptation of *R. electrica* to the on average higher acetate concentrations under open circuit conditions, which is not included in the model. The identified values for the lag phase factor in both the liquid phase ($k^{lag,lq,0}$) and in the biofilm ($k^{lag,bf,0}$), and $f_{0,bf,0}$ were at the upper boundary of the allowed parameter intervals. Since the major aim of the model was a description of the main conversion steps and no detailed explanation of the initial adaptation process of the bacteria, this was accepted without any further refinement of the model.

Finally, the effects of different strategies for improving the CE of our bioelectrochemical co-culture were predicted using the simulation model. Three promising approaches have been identified (Figure 6). First, the genetic inactivation of the acetate consumption pathway in *R. electrica* should increase the CE from 20.8% to 38.5% (Figure 6a). When acetate is only consumed by the *G. sulfurreducens* biofilm, a higher amount of this metabolite should accumulate in the liquid phase, which then allows the biofilm to continue growing and producing current.

Secondly, another way to achieve higher CEs should arise from an increase of the initial biofilm biomass via pre-cultivating *G. sulfurreducens* on anodes (Figure 6b). For an initial

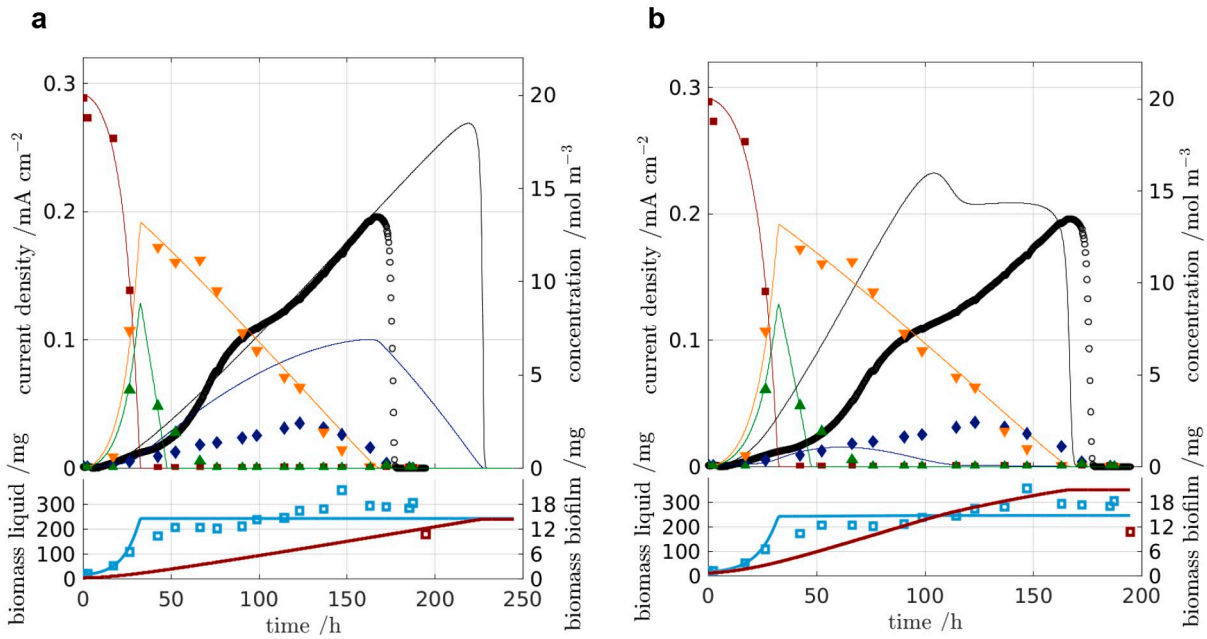

Figure 6. Simulated development of current density and metabolite concentrations without endogenous acetate consumption (a), and for a pre-cultivated anode (b). Shown are the current densities (○), the liquid phase biomass obtained from the optical densities of planktonic cells determined at 600 nm (□), the biofilm biomass determined at the end of the experiment (□), and the measured concentrations of glycerol (■), acetate (♦), formate (▲) and ethanol (▼). The lines denote simulated data. The symbols show the experimental data points for comparison.

biomass of 0.8 mg, the simulations show that the biofilm directly consumes the produced acetate so that only a low amount of acetate accumulates in the liquid phase and endogenous acetate consumption is suppressed. This second approach should lead to an increase of the CE up to 31.8%. Further, a high current density should be reached much earlier with a pre-cultivated anode (100 hours vs. 170 hours). Anyway, when pre-cultivated biofilms at the anodes are used, the overall current density is only limited by the conversion of ethanol to acetate.

Thirdly, the ratio of electrode surface area to reactor volume could be increased for example by using a high surface area material such as a carbon brush. In Figure S11 the simulated course of the cultivation is shown for a doubled anode surface area. Based on the simulation results, this strategy would increase the CE to 29.5%.

A fourth theoretical approach could be to force a direct conversion of glycerol into acetate without the production of ethanol by disrupting the *adhE* gene, encoding the alcohol dehydrogenase. This simulation was not taken into account here as *E. coli* mutants lacking the respective alcohol dehydrogenase did not show any growth.[45]

In summary, the simulation results presented above demonstrate that the competition for acetate between *R. electrica* and *G. sulfurreducens* limited the overall current production. Two approaches to increase the overall efficiency were deduced.

3. Conclusions

The successful combination of *R. electrica* with *G. sulfurreducens* for efficient bioelectrochemical current production using glycerol as substrate is only the first step towards the design of more complex artificial bacterial communities for electrical power generation. The corresponding mathematical model of the overall process allowed us to simulate different optimization conditions. In the next step this knowledge-based approach, combining genome-based information with experimental physiological data, for the prediction of metabolic interactions will be employed for the design of even more complex bacterial communities utilizing different cheap electron acceptors at the same time. The ultimate goal is the establishment of a construction kit composed of different bacterial species and corresponding process condition for the utilization of complex waste materials in bioelectrochemical for the generation of electrical power.

Experimental Section

Electrochemical setup and analysis

Enrichment cultures from wastewater

The enrichment cultures from wastewater were cultivated in a three-electrode single-chamber half-cell with a working volume of 500 mL. Graphite plates (CP-Graphitprodukte GmbH, Germany) were used as working (3 cm × 3 cm, area: 18 cm^2) and counter (4 cm × 4 cm, area: 32 cm^2) electrodes. Graphite electrodes were polished with 240-grit sandpaper and washed thoroughly with deionized water before assembling. The electrochemical reactors were sealed with conical silicon plugs (Deutsch & Neumann GmbH, Germany). A central embedded cable connector functioned as port for the reference electrode. The graphite electrodes were passed through the silicon plug by stainless steel wires. The electrochemical reactors were autoclaved with all components except for the reference electrode which was sterilized by using a 70% ethanol solution.

Co-culture of *G. sulfurreducens* and *R. electrica*

All co-culture experiments were performed in a three-electrode single-chamber half-cell with a working volume of 500 mL. Graphite plates (CP-Graphitprodukte GmbH, Germany) were used as working (4.5 cm × 5.5 cm, area: 49.5 cm^2) and counter (5.5 cm × 5.5 cm, area: 60.5 cm^2) electrodes and prepared as described above. The graphite electrodes were screwed onto a PTFE lid that also contained a butyl rubber stopper as sample port and pressure relief valve. A butyl pad, mounted under the PTFE lid, enabled gas tight outlets of all (screwing) ports and ensured anoxic conditions. The electrochemical reactors were autoclaved with all components except for the reference electrode which was sterilized by using a 70% ethanol solution.

For all bioelectrochemical cultivations of the enriched cultures from wastewater and the co-cultures of *G. sulfurreducens* and *R. electrica* an anode potential of 0.2 V vs. Ag/AgCl (SE11 reference electrode, sat. KCl, Xylem Analytics, Germany) was applied. Chronoamperometry was performed with intervals of 60 s using a MPG-2 potentiostat (Bio-Logic Science Instruments, France).

Cultivation media and methods

Cultivation media

All bioelectrochemical experiments were performed under anoxic conditions as biological triplicates. The sterilized defined cultivation medium (500 mL) with 20 mM pure glycerol as electron donor contained in a basal solution 12.5 mL vitamin solution and 12.5 mL trace element solution. The basal solution according to Kim *et al.* (2005) was composed of 310 mg L^{-1} NH_4Cl, 130 mg L^{-1} KCl, 2.69 g L^{-1} $NaH_2PO_4 \cdot H_2O$ and 4.33 g L^{-1} Na_2HPO_4.[15] The vitamin solution according to Balch *et al.* (1979) was composed of 2 mg L^{-1} biotin, 2 mg L^{-1} folic acid, 10 mg L^{-1} pyridoxine hydrochloride, 5 mg L^{-1} thiamine hydrochloride, 5 mg L^{-1} riboflavin, 5 mg L^{-1} nicotinic acid, 5 mg L^{-1} DL-calcium pantothenate, 100 µg L^{-1} vitamin B_{12}, 5 mg L^{-1} *p*-aminobenzoic acid and 5 mg L^{-1} lipoic acid.[51] The trace element solution contained 1.5 g L^{-1} nitrilotriacetic acid, 3 g L^{-1} $MgSO_4 \cdot 7\ H_2O$, 500 mg L^{-1} $MnSO_4 \cdot 2\ H_2O$, 1 g L^{-1} NaCl, 100 mg L^{-1} $FeSO_4 \cdot 7\ H_2O$, 100 mg L^{-1} $CoCl_2$, 100 mg L^{-1} $CaCl_2 \cdot 2\ H_2O$, 130 mg L^{-1} $ZnSO_4$, 100 mg L^{-1} $CuSO_4 \cdot H_2O$, 100 mg L^{-1} $AlK(SO_4)_2$, 100 mg L^{-1} H_3BO_3, 10 mg L^{-1} $Na_2MoO_4 \cdot 2\ H_2O$, 300 µg L^{-1} $Na_2SeO_3 \cdot 5\ H_2O$ and 30 mg L^{-1} $NiCl_2 \cdot 6\ H_2O$. This minimal medium was used for the enrichment of wastewater-derived biofilms and for the co-culture of *G. sulfurreducens* and *R. electrica* (pre-cultures and electrochemical cultivations).

Bioelectrochemical enrichment from wastewater

The electrochemical reactors were inoculated with 5% (v/v) primary wastewater from the wastewater treatment plant Steinhof, Braunschweig, Germany. All experiments were performed at 35 °C as batch cultures and stirred at 250 min^{-1} using a magnetic bar to

ensure a thorough distribution of substrate and nutrients. These primary biofilms were scraped off after four current cycles and used together with 10% (v/v) culture broth to inoculate two times new bioelectrochemical reactors resulting in secondary and tertiary biofilms. In addition, samples for the amplicon RNA sequencing were taken at these time points.

Establishing co-culture of *G. sulfurreducens* and *R. electrica*

G. sulfurreducens PCA^T (DSM 12127^T) and *R. electrica* 1GB^T (DSM 102253^T) were obtained from the Leibniz Institute – German Collection of Microorganisms and Cell Cultures (DSMZ, Germany). Both strains were pre-cultured as pure cultures under anoxic conditions in 100 mL serum bottle flasks sealed airtight with butyl rubber stoppers and filled with 50 mL minimal medium (described above). Pure cultures of *G. sulfurreducens* were supplemented with 10 mM acetate as electron donor and 40 mM fumarate as electron acceptor. Pure cultures of *R. electrica* were grown anaerobically in the presence of 20 mM glycerol and 56 mM nitrate. After reaching the mid-exponential growth phase, pre-cultures of both species were harvested separately via centrifugation (4 °C; 15 min; 1,250 g) and re-suspended individually in basal solution. For co-cultivations, the minimal medium described above was used supplemented with 20 mM glycerol as sole electron donor. The electrochemical reactor was inoculated with a final OD_{600} of 0.1 of each organism. Anoxic conditions were provided by flushing the media before and after inoculation with nitrogen. All experiments were performed at 30 °C as batch cultures and stirred at 250 min^{-1} using a magnetic bar to ensure a thorough distribution of substrate and nutrients.

Determination of growth parameters

The optical density of *G. sulfurreducens* and *R. electrica* was measured at 600 nm (OD_{600}). A correlation between OD_{600} and cell dry weight (CDW) was performed for pure cultures, respectively. For *G. sulfurreducens*, an OD_{600} of 0.5 correlates to a CDW of 0.2487 g L^{-1} ($R^2 = 0.98$) and for *R. electrica* an OD_{600} of 0.5 correlates to a CDW of 0.2231 g L^{-1} ($R^2 = 0.94$). For the first 4 samples 2 mL each were taken and for the following samples 1.5 mL. After taking the last sample of the cultivation, the biomass of the anode of each reactor was determined by thoroughly removing the biofilm and mixing the recovered cells with 10 mL basal solution, resulting in a homogenous cell suspension. After measuring the OD_{600} of these suspensions, the mean value of the OD_{600} from the co-cultures under open circuit conditions was used as blank for the cell suspension under closed circuit conditions, which originated from the anodic biofilm of the cultivation. It was observed that neither *G. sulfurreducens* nor *R. electrica* can form a biofilm on the anode under open circuit conditions and that the measured OD_{600} was solely caused by planktonic *R. electrica* cells. The CDW of cells attached to the anode was then calculated using the OD-CDW correlation factor for *G. sulfurreducens*.

Substrate and metabolite analysis

High performance liquid chromatography (HPLC) was used to analyze extracellular concentrations of glycerol and organic acids. Samples were centrifuged (4 °C; 5 min; 15,700 g) and the supernatant was filtered using a 0.2 µM syringe filter. Glycerol was separated by chromatography on a MetaCarb 87 C column (Agilent Technologies, Inc., USA) operating at 85 °C with ultra-pure H_2O as the mobile phase and at a flow rate of 0.6 mL min^{-1}. Glycerol concentrations were then determined using a LaChrom Elite refractive index detector (Hitachi, High Technologies America, Inc, USA). Organic acids were separated by chromatography on an Aminex HPX-87H (Bio-Rad Laboratories GmbH, Germany) column at 45 °C with 12 mM H_2SO_4 as the mobile phase using a flow rate of 0.5 mL min^{-1}. Organic acids were detected by a LaChrom Elite RI detector and a LaChrom Elite Diode Array Detector (Hitachi, High Technologies America, Inc, USA) at a wavelength of 210 nm.

V3 amplicon sequencing

The bacterial communities of primary, secondary and tertiary biofilms and corresponding planktonic cells after four current cycles were analyzed by partial 16S rRNA sequencing. Briefly, after reverse transcription of RNA to cDNA, amplicons of the V3 region of the 16S rRNA were prepared and sequenced on the Illumina HiSeq 2500 (Illumina, San Diego, CA, U.S.). Details on RNA extraction, amplicon preparation of the V3 region of the 16S rRNA gene and bioinformatics interpretation were described previously.[13] In total, about 500,000 V3 amplicon reads were obtained per sample. Raw read data has been submitted to the European Nucleotide Archive, study accession number PRJEB36918 (http://www.ebi.ac.uk/ena/data/view/PRJEB36918).

Acknowledgements

The authors acknowledge financial support of the NTH-research group ElektroBak by the State of Lower Saxony. We acknowledge support by the German Research Foundation and the Open Access Publication Funds of the Technische Universität Braunschweig. The authors also thank Prof. Uwe Schröder (Institute of Environmental and Sustainable Chemistry, TU Braunschweig) for helpful discussions.

Conflict of Interest

The authors declare no conflict of interest.

Keywords: microbial electrolysis cell · modelling and simulation · glycerol · oxidation · electrochemistry

[1] H. Liu, R. Ramnarayanan, B. E. Logan, *Environ. Sci. Technol.* **2004**, *38*, 2281–2285.
[2] J. Niessen, U. Schröder, F. Scholz, *Electrochem. Commun.* **2004**, *6*, 955–958.
[3] Y. Zuo, P.-C. Maness, B. E. Logan, *Energy Fuels* **2006**, *20*, 1716–1721.
[4] C. A. G. Quispe, C. J. R. Coronado, J. A. Carvalho Jr, *Renewable Sustainable Energy Rev.* **2013**, *27*, 475–493.
[5] F. Yang, M. A. Hanna, R. Sun, *Biotechnol. Biofuels.* **2012**, *5*, 13.
[6] S. Hu, X. Luo, C. Wan, Y. Li, *J. Agric. Food Chem.* **2012**, *60*, 5915–5921.
[7] Y.-P. Liu, Y. Sun, C. Tan, H. Li, X.-J. Zheng, K.-Q. Jin, G. Wang, *Bioresour. Technol.* **2013**, *142*, 384–389.
[8] T. Chookaew, P. Prasertsan, Z. J. Ren, *Nat. Biotechnol.* **2014**, *31*, 179–184.
[9] A. Tremouli, T. Vlassis, G. Antonopoulou, G. Lyberatos, *Waste Biomass Valorization* **2016**, *7*, 1339–1347.
[10] T. Chookaew, P. Prasertsan, Z. J. Ren, *Nat. Biotechnol.* **2014**, *31*, 179–184.
[11] Y. Sharma, R. Parnas, B. Li, *Int. J. Hydrogen Energy.* **2011**, *36*, 3853–3861.
[12] M. Nishioka, H. Den, T. Noda, K. Sugiura, *ECS Trans.* **2018**, *83*, 137–143.
[13] F. Kubannek, C. Moß, K. Huber, J. Overmann, U. Schröder, U. Krewer, *Front. Energy Res.* **2018**, *6*, 125.
[14] A. Q. Guimarães, J. J. Linares, *J. Electrochem. Soc.* **2014**, *161*, F125–F132.
[15] J. R. Kim, B. Min, B. E. Logan, *Appl. Microbiol. Biotechnol.* **2005**, *68*, 23–30.
[16] A. Baudler, S. Riedl, U. Schröder, *Front. Energy Res.* **2014**, *2*, 260.

[17] F. Caccavo, D. J. Lonergan, D. R. Lovley, M. Davis, J. F. Stolz, M. J. McInerney, *Appl. Environ. Microbiol.* **1994**, *60*, 3752–3759.
[18] K. Venkateswaran, D. P. Moser, M. E. Dollhopf, D. P. Lies, D. A. Saffarini, B. J. MacGregor, D. B. Ringelberg, D. C. White, M. Nishijima, H. Sano, J. Burghardt, E. Stackebrandt, K. H. Nealson, *Int. J. Syst. Bacteriol.* **1999**, *49 Pt 2* (1 999), 705–24.
[19] J. M. Flynn, D. E. Ross, K. A. Hunt, D. R. Bond, J. A. Gralnick, *mBio* **2010**, *1*, e00190–10.
[20] P. V. Dantas, S. Peres, G. M. Campos-Takaki, C. E. La Rotta, *J. Electrochem. Soc.* **2013**, *160*, G142–G148.
[21] A. Reiche, K. M. Kirkwood, *Bioresour. Technol.* **2012**, *123*, 318–323.
[22] K. Sturm-Richter, F. Golitsch, G. Sturm, E. Kipf, A. Dittrich, S. Beblawy, S. Kerzenmacher, J. Gescher, *Bioresour. Technol.* **2015**, *186*, 89–96.
[23] M. Y. Kim, C. Kim, S. K. Ainala, H. Bae, B. H. Jeon, S. Park, J. R. Kim, *Bioelectrochemistry.* **2019**, *125*, 1–7.
[24] V. R. Nimje, C. Y. Chen, C. C. Chen, H. R. Chen, M. J. Tseng, J. S. Jean, Y. F. Chang, *Bioresour. Technol.* **2011**, *102*, 2629–2634.
[25] A. M. Speers, J. M. Young, G. Reguera, *Environ. Sci. Technol.* **2014**, *48*, 6350–6358.
[26] P. A. Selembo, J. M. Perez, W. A. Lloyd, B. E. Logan, *Int. J. Hydrogen Energy.* **2009**, *34*, 5373–5381.
[27] C. Kim, Y. E. Song, C. R. Lee, B.-H. Jeon, J. R. Kim, *J. Ind. Microbiol. Biotechnol.* **2016**, *43*, 1397–1403.
[28] F. Li, C. Yin, L. Sun, Y. Li, X. Guo, H. Song, *Biotechnol. J.* **2018**, *13*, 1–8.
[29] A. M. Speers, G. Reguera, *Appl. Environ. Microbiol.* **2012**, *78*, 437–444.
[30] K. P. Nevin, H. Richter, S. F. Covalla, J. P. Johnson, T. L. Woodard, A. L. Orloff, H. Jia, M. Zhang, D. R. Lovley, *Environ. Microbiol.* **2008**, *10*, 2505–2514.
[31] S. Thiel, B. Bunk, C. Spröer, J. Overmann, D. Jahn, R. Biedendieck, *Microbiol. Res.* **2019**, *8*.
[32] Y. Feng, Q. Yang, X. Wang, Y. Liu, H. Lee, N. Ren, *Bioresour. Technol.* **2011**, *102*, 411–415.
[33] N. Montpart, L. Rago, J. A. Baeza, A. Guisasola, *Water Res.* **2015**, *68*, 601–615.
[34] F. Kubannek, C. Moß, K. Huber, J. Overmann, U. Schröder, U. Krewer, *Front. Energy Res.* **2018**, *6*, 2–11.
[35] K. Y. Kim, K. J. Chae, M. J. Choi, F. F. Ajayi, A. Jang, C. W. Kim, I. S. Kim, *Bioresour. Technol.* **2011**, *102*, 4144–4149.
[36] Z. M. Summers, H. E. Fogarty, C. Leang, A. E. Franks, N. S. Malvankar, D. R. Lovley, *Science* **2010**, *330*, 1413–1415.
[37] A.-E. Rotaru, P. M. Shrestha, F. Liu, T. Ueki, K. Nevin, Z. M. Summers, D. R. Lovley, *Appl. Environ. Microbiol.* **2012**, *78*, 7645–7651.
[38] M. S. Kim, Y. J. Lee, *Int. J. Hydrogen Energy.* **2010**, *35*, 13028–13034.
[39] C. I. Torres, A. K. Marcus, B. E. Rittmann, *Biotechnol. Bioeng.* **2008**, *100*, 872–881.
[40] A. Kato Marcus, C. I. Torres, B. E. Rittmann, *Biotechnol. Bioeng.* **2007**, *98*, 1171–1182.
[41] D. Sun, J. Chen, H. Huang, W. Liu, Y. Ye, S. Cheng, *Int. J. Hydrogen Energy.* **2016**, *41*, 16523–16528.
[42] J. Meng, Z. Xu, J. Guo, Y. Yue, X. Sun, *PLoS One.* **2013**, *8*, e73907.
[43] B. A. Methé, K. E. Nelson, J. A. Eisen, I. T. Paulsen, W. Nelson, J. F. Heidelberg, D. Wu, M. Wu, N. Ward, M. J. Beanan, R. J. Dodson, R. Madapu, L. M. Brinkac, S. C. Daugherty, R. T. DeBoy, Durkin, A. S. Durkin, M. Gwinn, J. F. Kolonay, S. A. Sullivan, D. H. Haft, J. Selengut, T. M. Davidsen, N. Zafar, O. White, B. Tran, C. Romero, H. A Forberger, J. Weidman, H. Khouri, T. V. Feldblyum, T. R. Utterback, S. E. Van Aken, D. R. Lovley, C. M. Fraser, *Science.* **2003**, *302*, 1967–9.
[44] G. Reguera, *Proc. Natl. Acad. Sci. USA* **2018**, *115*, 5632–5634.
[45] A. Murarka, Y. Dharmadi, S. S. Yazdani, R. Gonzalez, *Appl. Environ. Microbiol.* **2008**, *74*, 1124–35.
[46] J. J. Heijnen, in *Encycl. Bioprocess Technol.*, John Wiley & Sons, Inc., Hoboken, NJ, USA **2002**.
[47] H. Richter, K. P. Nevin, H. Jia, D. a Lowy, D. R. Lovley, L. M. Tender, *Energy Environ. Sci.* **2009**, *2*, 506.
[48] L. Peng, X.-T. Zhang, J. Yin, S.-Y. Xu, Y. Zhang, D.-T. Xie, Z.-L. Li, *Electrochim. Acta.* **2016**, *191*, 743–749.
[49] I. A. M. Swinnen, K. Bernaerts, E. J. J. Dens, A. H. Geeraerd, J. F. Van Impe, *Int. J. Food Microbiol.* **2004**, *94*, 137–159.
[50] F. Kubannek, U. Krewer, *Chemie* **2019**, *91*, 856–864.
[51] W. E. Balch, G. E. Fox, L. J. Magrum, C. R. Woese, R. S. Wolfe, *Microbiol. Rev.* **1979**, *43*, 260–96.

Manuscript received: January 7, 2020
Revised manuscript received: March 3, 2020